Self-induced slow-fast dynamics and swept bifurcation diagrams in weakly desynchronized systems

Michael A. Zaks, Eun-Hyoung Park*, Jürgen Kurths
Institute of Physics, Potsdam University, PF 601553, D-14415 Potsdam Germany

In systems close to the state of phase synchronization, the fast timescale of oscillations interacts with the slow timescale of the phase drift. As a result, "fast" dynamics is subjected to a slow modulation, due to which an autonomous system under fixed parameter values can imitate repeated bifurcational transitions. We demonstrate the action of this general mechanism for a set of two coupled autonomous chaotic oscillators and for a chaotic system perturbed by a periodic external force. In both cases, the Poincaré sections of phase portraits resemble bifurcation diagram of a logistic mapping with time-dependent parameter.

PACS numbers: 05.45-a, 05.45.Xt

In real physical problems external parameters can only approximately be viewed as constant. A gradual variation of parameters remains harmless as long as it does not produce qualitative changes in the behavior of the system. However it may happen that a time-dependent parameter crosses a critical value beyond which the attracting state changes. The interaction of the slow parameter variation with the fast rate of motions in the phase space is the cause of phenomena known under the name of "dynamic bifurcations" (see e.g. [1]). One of its peculiarities is the bifurcation delay: the system fails to "notice" the onset of instability and tracks for a long time the unstable branch of states, before exhibiting a swift transition to a new state. The influence of a slow monotonic parameter variation ("sweep") on the sequence of period-doubling bifurcations was described in [2] and later investigated in detail in [3]. Although the obtained bifurcation diagrams resemble the familiar diagram of a logistic mapping [4,5], some differences arise, due to the inevitable presence of transients. With respect to the usual period-doubling scenario, a certain similarity between the sweep and the action of noise has been established: under a non-zero sweep rate only a finite number of doubling bifurcations is observable. Theoretical predictions were confirmed by experiments on electronic circuits and lasers with monotonically varied characteristics [6,7].

Existing examples of dynamic bifurcations employ the explicit slow variation of parameter. In this paper, we report on a mechanism which enables sequences of dynamic bifurcations in autonomous systems with fixed parameters and in systems which are forced at fast timescales. For the attractors of such systems, the Poincaré sections look like bifurcation diagrams.

We consider dynamics close to the regime of phase synchronization. The notion of phase synchronization for chaotic systems extends the idea of synchronization in coupled periodic oscillators: it is based on the decomposition of a chaotic signal into the slowly varying amplitude and rapidly rotating phase. As shown in [8], in weakly coupled chaotic systems the onset of a certain partial order is possible: amplitudes of oscillations in individual subsystems remain largely uncorrelated, whereas their phases synchronize; the mean frequencies of chaotic motions in subsystems become commensurate. Phase synchronization precedes the "complete synchronization" observed under very strong coupling, when subsystems display identical dynamics [9–11]. For simplicity, here we restrict ourselves to the "main resonance" when the mean frequencies of subsystems are locked in the 1:1 ratio. In the synchronized state, the difference between the phases of the subsystems remains confined within a finite range. Just outside the domain of phase synchronization in the parameter space, a certain intermittency is observed: long time intervals at which the phase difference is confined, alternate with intervals of phase drift [12,13].

Although the phase itself is a "fast" variable, variations of phase difference occur on a slow timescale and slowly modulate the amplitude. Until now, no attention seems to be paid to the fact that this modulation may result in dynamic bifurcations and, since the phase is a cyclic variable, imitate repetitive sweeps back and forth through bifurcation sequences even in the completely time-independent setup. This effect should be especially well visible when one of the subsystems, if considered alone, is close to the accumulation point of a bifurcation scenario, whereas the state of the second one is qualitatively robust against minor parameter perturbations. Below we illustrate this phenomenon with the help of two coupled autonomous oscillators, a periodically forced chaotic system and a two-dimensional map.

Our test objects are the textbook examples of chaotic dynamics. We start with two coupled nonidentical Rössler oscillators:

$$\begin{aligned} \dot{x}_{1,2} &= -y_{1,2} - z_{1,2} + \varepsilon(x_{2,1} - x_{1,2}) \\ \dot{y}_{1,2} &= x_{1,2} + A_{1,2}y_{1,2} \\ \dot{z}_{1,2} &= B + z_{1,2}(x_{1,2} - C) \end{aligned} \tag{1}$$

Following the original work of Rössler [14], we fix $B = 0.2$ and $C = 10$; the value $A_1 = 0.11$ ensures chaotic motion of the separate oscillator whereas $A_2 = 0.05$ corresponds to a periodic state. The parameter ε characterizes the strength of the coupling. Since projection of the chaotic motion onto the xy plane of each subsystem looks like counterclockwise rotations around the origin with fluctuating amplitude and period, it is convenient to introduce two phases as lifts of angular coordinates: $\Psi_{1,2} = \arctan(y_{1,2}/x_{1,2}) + \frac{\pi}{2}\,\mathrm{sign}(x_{1,2})$ [8].

Under a very weak coupling, both the amplitudes and the phases of nonidentical interacting Rössler oscillators are unlocked. An increase of the coupling coefficient ε beyond the small threshold value $\varepsilon_{\rm ps}$ leads to the onset of phase synchronization [8]. In the following we adjust ε slightly below this threshold which for the chosen set of $A_{1,2}, B, C$ equals $\varepsilon_{\rm ps} = 0.016637516$.

Isosurfaces of either of the phases are natural candidates for Poincaré surfaces; we take for this aim the hyperplane $y_1 = 0$ and sample the points in which the orbit intersects this plane "from above" ($\dot{y_1} < 0$). The dynamics of phase difference between two subsystems is represented by values of Ψ_2 computed at the moments of intersection with the Poincaré plane (Fig. 1a). In accordance with the theory [12,13], long ($\sim 800\div 1000$ iterations) plateaus are interrupted by epochs of phase drift; typical length of the latter is $60\div 80$ iterations. The Poincaré section of the orbit projected onto the cylinder x_1, $\Psi_2(\mathrm{mod}2\pi)$ is shown in Fig. 1b [15]. As time goes on, the cylindrical surface is traversed from right to the left; when the left border is reached, the imaging point reappears on the right side, etc.

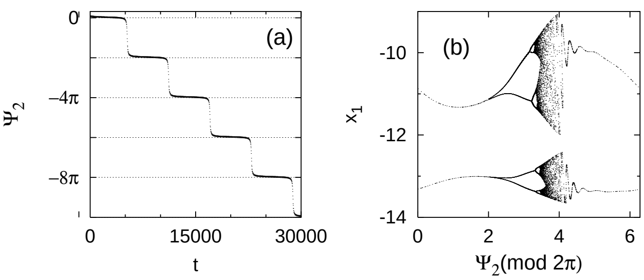

FIG. 1. Two coupled Rössler oscillators: Eq.(1) with $A_1 = 0.11$, $A_2 = 0.05$, $B = 0.2$, $C = 10$, $\varepsilon = 0.01660$.
(a) Time evolution of the phase difference;
(b) Poincaré section of a trajectory on the plane $y_1 = 0$.

At first sight, the set in Fig. 1b reminds a part of the bifurcation diagram for the logistic map. At a closer look, we notice the fingerprints of dynamic bifurcations [2,3]: compared to the conventional diagrams of [4,5] the forks near the bifurcation points are deformed, and only several bifurcations can be resolved. The motion is chaotic; however, in the segments which remind periodic windows of the bifurcation diagram, local Lyapunov exponents are negative. Strong local contraction makes the corresponding part of the set so squeezed that its transverse structure remains below the level of numerical resolution. (The equations were integrated by recurrent expansions into the Taylor series of the 25th order with variable timestep and relative error per step 10^{-17}. The width of the "stripes" in the periodic windows does not exceed 10^{-13}; this strong contraction is a characteristic feature of dynamic bifurcations, provided the parameter sweep is slow enough [1,3]). Imitated bifurcations correspond to the "backward sweep" of the parameter: ... period 8 $\to$ period 4 $\to$ period 2. In the part of the set which corresponds to the forward sweep, sequence of doublings is not observed due to the strong delay of the bifurcation in the period-2 branch. Slowly traversing the segment with local contraction, the orbits track this branch so closely, that later, when the branch is no more attracting, they remain in its vicinity rather long; by the time when they finally depart, the bifurcation diagram already reaches a chaotic stage.

Imitated bifurcation scenarios can be also recovered in oscillators in which intrinsic chaotic dynamics interacts with an external periodic force. Analysis of phase synchronization in driven chaotic systems showed that under forcing with period close to the mean period of chaotic oscillations, the phase of chaotic motion could be captured by the phase of the force [16]. To enable this, for a given amplitude of the force the driving frequency should lie within a certain range. Just outside this range, long time intervals in which the phase of the system follows the phase of the force, alternate with epochs where two phases drift apart. The latter drift can be rather slow: it may take hundreds of periods of external force in order to increase the phase difference by $\sim 2\pi$. Fast oscillations of the system on the background of this slow drift can provide conditions for dynamic bifurcations.

As an example, consider the periodically driven Lorenz equations;

$$\begin{aligned} \dot{x} &= \sigma(y - x), \quad \dot{y} \;=\; rx - y - xz, \\ \dot{z} &= xy - bz + E\cos(\Omega t) \end{aligned} \qquad (2)$$

Here, σ=10 and $b = 8/3$ are the values from the original paper of Lorenz [17], E and Ω are, respectively, amplitude and frequency of the external force. The value of r is fixed at 215.25; in the autonomous system this corresponds to the chaotic state and lies close to the accumulation point of the period-doubling sequence at $r = 215.364$ [5].

In the absence of forcing ($E = 0$) the mean frequency of chaotic motion in Eq.(2) equals 25.25552 $[t]^{-1}$ in dimensionless units. An external periodic action at close values of Ω can entrain the phase of the system. Onset of phase synchronization in Eq.(2) and analysis of this state were described in [18]; in contrast, our current interest lies in slightly *desynchronized* motions. For $E = 1.5$ phase synchronization occurs in the interval Ω_L=25.24004< Ω < Ω_R=25.27308. We take the values of Ω outside this interval. For the Poincaré section we choose the plane $z = r - 1$ and mark the places where an orbit intersects this plane from above. The coordinates

x and y of the intersection point characterize the amplitude of the motion; due to the strong contraction, either of these coordinates suffices for practical reasons. The remaining information is provided by the phases of the system and the driving force. At the moment t_j of the j-th intersection of the orbit with the Poincaré plane, the former phase, by definition, is set to $2\pi j$ (for the discussion on the estimation of phase in the Lorenz equations see [16,18]), and the phase ψ of external force equals Ωt_j.

Typical examples of the evolution of the phase difference between the force and the system just outside the region of phase synchronization are shown in Fig. 2a,c. The respective Poincaré sections in coordinates x, $\psi(\text{mod}2\pi)$ are plotted in Fig. 2b,d. Since for $\Omega < \Omega_L$ the average frequency of driven chaotic motion exceeds the frequency of the force, the plot in Fig. 2b is traversed from left to the right. For $\Omega > \Omega_R$ the force turns out to be faster, therefore Fig. 2d is traversed from right to the left.

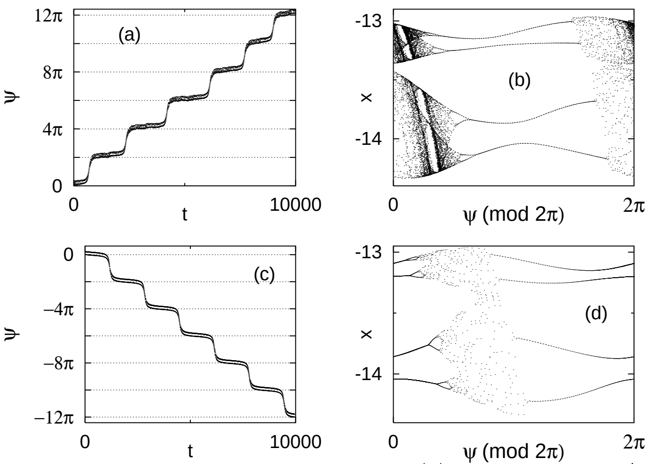

FIG. 2. Forced Lorenz equations (2) at σ=10, b=8/3, r=215.25, E=1.5; (a),(b): Ω=25.2396; (c),(d): Ω=25.2735. (a),(c) Time evolution of the phase difference; (b),(d) Poincaré section on the plane $z = r - 1$.

Again, the Poincaré sections resemble dynamic bifurcation diagrams. Along with the main doubling sequence, the "window" of period 6 is distinctly seen in Fig. 2b. Increase of the forcing leads to the growth of the modulation depth which, in its turn, results in the imitation of a larger piece of the bifurcation diagram: cf. Fig. 3 where not only the pieces of "stable period 4 and 8" but also pieces of "period 2" are recognizable.

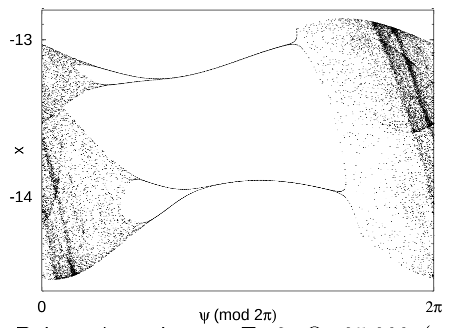

FIG. 3. Poincaré section at E=3, Ω=25.222 (parameters σ, b, r as in Fig. 2).

To get a simple but still efficient model of dynamics on the Poincaré plane, consider a two-dimensional mapping. The participating variables are the amplitude of the motion u (analog for x or y from Eq. (2)) and the phase ψ of the external force at the moment of intersection of the orbit with the plane. The intrinsic dynamics of u is governed by a quadratic map; the contribution of the weak force is proportional to its amplitude ϵ:

$$u_{n+1} = \mu - u_n^2 + \epsilon \sin \psi_n \qquad (3)$$

The value of phase ψ_{n+1} equals $\psi_n + \omega \tau_n$ where ω is the forcing frequency, and the return time τ_n is the interval between the n-th and the $n+1$-th intersection of the Poincaré surface. For the attractors of both the Lorenz equations at large R and the Rössler equations, the return time very weakly depends on the position on the surface. Approximating this dependence by a linear function with a small slope, the lowest order in ϵ yields:

$$\psi_{n+1} = \psi_n + \omega\,(a + b u_n + \epsilon d \sin(\psi_n + \psi_0)) \qquad (4)$$

Here a, b, d, and ψ_0 are parameters. To ensure proximity to phase synchronization, ωa should be close to 2π. The mapping (3,4) combines a quadratic map with a circle map whose rotation number is close to 1.

For the map $u_{n+1} = \mu - u_n^2$ the accumulation point of a period-doubling scenario lies at $\mu = 1.401155189$. At close values of μ and a moderate ϵ it is possible to have in (3,4) chaotic attractors with values of $\psi\,(\text{mod}2\pi)$ localized inside the narrow strip; this corresponds to the state of phase synchronization. By fixing e.g. $\mu = 1.41$, $\epsilon = 0.25$, $a = 6.29$, $b = 0.025$, $d = 0.1$ and $\psi_0 = \pi/2$ we observe that this state exists under $\omega_L = 0.992891 < \omega < \omega_R = 1.000801$. As seen in Fig. 4, a plot of a typical orbit at a value of ω just outside this "synchronization range", displays apparent similarity to Fig. 3 [19].

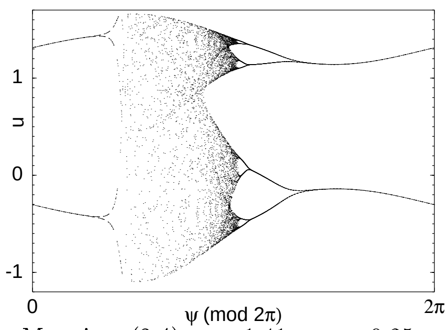

FIG. 4. Mapping (3,4): μ=1.41, $\epsilon = 0.25$, $a = 6.29$, $b = 0.025$, $d = 0.08$, $\psi_0 = \pi/2, \omega = 1.001$.

Let us have a closer look at the details of the evolution in the phase space. For Eq. (2) at $E = 1.5$ the motion is chaotic in the left part of the interval $\Omega_L < \Omega < \Omega_R$ and periodic near its right boundary. On both borders phase desynchronization is caused by tangent bifurcations of periodic orbits which intersect the Poincaré surface 4 times. At Ω_L two unstable periodic orbits coalesce, provoking an attractor-repeller collision [12,13]. At Ω_R the stable limit cycle is destroyed by a saddle-node bifurcation. In both cases, a kind of a "channel" is formed in the phase space, allowing the orbits to escape from the phase-synchronized state. The motion along this channel is slow: basing on the mapping (3,4) and the pattern from Fig. 4, duration T_d of the drift stage can be roughly estimated as $T_d \sim 2\pi/|\omega(a + b/2) - 2\pi|$ iterations. Notably, the drift velocity cannot be made arbitrarily small by tuning the force: both for $\omega \to \omega_R$ and $\omega \to \omega_L$, T_d remains finite. On the contrary, the average length T_s of a synchronized epoch grows unboundedly on approaching either of the endpoints from outside. The scaling laws which characterize this growth can be of two kinds: near the endpoint $\omega_{\rm ar}$ at which an attractor-repeller collision happens, T_s diverges as $\exp(\text{const}/\sqrt{|\omega - \omega_{\rm ar}|}\,)$ [12], whereas the saddle-node bifurcation at $\omega_{\rm sn}$ imposes the usual scaling law of the type-I intermittency: $T_s \sim |\omega - \omega_{\rm sn}|^{-1/2}$ [20]. In fact, the same scaling holds for the plateaus in Fig.1(a), since for the empoyed values of $A_{1,2}, B$ and C the transition in Eq.(1) at $\varepsilon = \varepsilon_{\rm ps}$ is a saddle-node bifurcation.

Increase of the distance in the parameter space from the borders of region of phase synchronization affects only weakly the duration of the drift stage, but the lifetime of nearly synchronized states becomes substantially shorter. In the course of this increase, saddle-saddle bifurcations destroy unstable periodic orbits and create new channels for the phase drift. As a result, the whole dynamical diagram on the Poincaré section becomes fuzzy, but its contours remain well recognizable.

A similar effect is produced by adding noise to the process: like in the case of explicitly imposed parameter sweep [3], minor details of the pattern become less distinct, and less dynamic bifurcations can be resolved. However, if the noise is not too strong, the typical outline of the diagram, with its merging curves, "windows" and dense clusters at the places of "attractor crises" persists. Therefore, we expect that this unusual sort of slow-fast dynamics under weak desynchronization of phases can be observed experimentally, e.g. by weakly disturbing the phase-synchronized regimes reported in [21].

The described phenomenon can be viewed as a kind of intermittency. The slow component which modulates the fast processes, is created by interaction of close frequencies: those of nonidentical Rössler oscillators in the first example, and those of the Lorenz system and the driving force in the second one. This reminds of the classical example, the generation of a beating frequency which slowly modulates the amplitude of fast quasiperiodic oscillations. In our case, however, most of the time the low-frequency component is virtually absent: its modulating action is recognizable only during the epochs of phase drift. Having reached a chaotic state with nearly synchronized phases of individual oscillators and coinciding individual frequencies, a system wanders along this state for a long time, until finally it finds itself in the opening of the "drift channel". In the course of the subsequent phase drift, the frequencies of both subsystems diverge, a low-frequency modulation sets on and eventually brings the system through the sequence of dynamic bifurcations back to the synchronized state. At this moment self-modulation is temporarily switched off, - and the cycle is repeated.

A natural question arises on the generality of the dynamic bifurcation diagrams in this context. Just outside the state of phase synchronization the phase drift is always slow, therefore the modulating effect should be generic. However, identification of dynamic bifurcations caused by this modulation can, in general, be a difficult task: if the interacting subsystems are in the state of well-developed chaos, the dynamic bifurcations are restricted to "chaos-chaos" transitions. If such transitions include crises associated with the abrupt change of the attractor size, the dynamic bifurcations should be visible. If, on the other hand, transitions result only in subtle changes in the geometry of chaotic attractors, it may be very difficult to recover these changes in the relatively short segments of phase drift.

As a final remark, we note that weak desynchronization and dynamic bifurcations may sometimes stand behind nonstationarity which manifests itself in the alternation of periodic and disordered behavior and is often encountered in datasets of experimental origin. Usually, nonstationarity is ascribed to variation of external conditions and action of noise; our first example shows that alternating regimes may be observed in a completely deterministic stationary setup.

Fruitful discussions with U. Feudel, A. Pikovsky and M. Rosenblum are gratefully acknowledged. Research of JK was supported by EC RTN 158.

[1] Dynamic Bifurcations, Lect. Notes Math. **1493**, edited by E. Benoît, Springer-Verlag, 1991.
[2] R. Kapral and P. Mandel, Phys. Rev. A **32**, 1076 (1985).
[3] C. Baesens, Physica D **53**, 319 (1991); Nonlinearity **8**, 179 (1995).
[4] P. Collet, J.-P. Eckmann, *Iterated Maps on the Interval as Dynamical System* (Birkhäuser, Basel, 1980).
[5] E. N. Lorenz, Ann. NY Acad. Sci. **357**, 282–291 (1980).
[6] B. Morris and F. Moss, Phys. Lett. A **118** 117 (1986).
[7] D. Dangoisse, P. Glorieux, and D. Hennequin, Phys. Rev. A **36**, 4775 (1987).
[8] M. G. Rosenblum, A. S. Pikovsky, J. Kurths, Phys. Rev. Lett. **76**, 1804 (1996).
[9] H. Fujisaka, T. Yamada, Prog. Theor. Phys. **69**, 32 (1983).
[10] A. S. Pikovsky, Z. Phys. B **55**, 149 (1984).
[11] L. M. Pecora, and T. L. Caroll, Phys. Rev. Lett. **64**, 821 (1990).
[12] A. S. Pikovsky, G. V. Osipov, M. G. Rosenblum, M. A. Zaks, J. Kurths, Phys. Rev. Lett. **79**, 47 (1997); A. S. Pikovsky, M. A. Zaks, M. G. Rosenblum, G. V. Osipov, J. Kurths, CHAOS **7**, 680 (1997).
[13] E. R. Rosa, E. Ott and M. H. Hess, Phys. Rev. Lett. **80**, 1642 (1998).
[14] O. E. Rössler, Phys. Lett. A **57**, 397 (1976).
[15] Of course, the qualitative picture persists if instead of Ψ_2 one of the "natural" variables (x_2, y_2) is used; the angular coordinate is preferred since in its terms the evolution is largely monotonic, and two different parts of the attractor do not overlap on the plot.
[16] A. S. Pikovsky, M. G. Rosenblum, G. V. Osipov, J. Kurths, Physica D **104**, 219 (1997).
[17] E. N. Lorenz, J. Atmos. Sci. **20**, 130 (1963).
[18] E.-H. Park, M. A. Zaks and J. Kurths, Phys. Rev. E **60**, 6627 (1999).
[19] Phase is defined up to a constant. This enables arbitrary horizontal translations of the plots.
[20] Y. Pomeau and P. Manneville, Commun. Math. Phys. **74**, 189 (1980).
[21] C. M. Ticos, E. Rosa, W. B. Pardo, J. A. Walkenstein and M. Monti, Phys. Rev. Lett. **85**, 2929 (2000); E. Allaria, F. T. Arecchi, A. Di Garbo, and R. Meucci, Phys. Rev. Lett. **86**, 791 (2001).